A Robust GPS/INS Kinematic Integrity Algorithm for Aircraft Landing

Alison Brown and Ben Mathews, *NAVSYS Corporation*

BIOGRAPHY

Alison Brown is the Chairman and Chief Visionary Officer of NAVSYS Corporation. She founded NAVSYS in 1986 and served as President and Chief Executive Officer until 2006. She has a PhD in Mechanics, Aerospace, and Nuclear Engineering from UCLA, an MS in Aeronautics and Astronautics from MIT, and an MA in Engineering from Cambridge University. She was a member of the GPS-3 Independent Review Team and the Interagency GPS Executive Board Independent Advisory Team, and is an Editor of GPS World Magazine. She is an ION Fellow and an Honorary Fellow of Sidney Sussex College, Cambridge

Ben Mathews is the manager of the Digital Signal Processing, Modeling, and Simulation Section at NAVSYS Corporation. His work includes the design and development of NAVSYS' advanced GPS systems including digital beam-steering receivers, GPS jammer geolocation systems, and bistatic spatial signal processing systems. He holds a MSEE from Virginia Tech.

ABSTRACT

Next generation GPS receivers will take advantage of Spatial processing from a Controlled Reception Pattern Antenna (CRPA) and Ultra-Tightly-Coupled (UTC) and Tightly–Coupled GPS/inertial signal processing to improve their robustness to interference and their performance in a multipath environment. This introduces the potential for failure modes to be introduced into the GPS solution from the Spatial processor, GPS signals or Inertial Measurement Units (IMUs). For high integrity applications such as non-precision approach or precision approach, the integrated GPS/Inertial receiver must be designed to perform fault detection and exclusion of any hazardously misleading information.

This paper describes the design of a GPS/Inertial Kinematic Integrity Monitor designed to monitor and detect for errors that affect the Kinematic Carrier Phase Tracking (KCPT) solution. This has been implemented and tested in NAVSYS' HAGR digital beam-forming receiver. Testing on the algorithm performance was performed using a high fidelity simulator designed for GPS wavefront simulation and GPS/inertial UTC testing based on NAVSYS' Advanced GPS Hybrid Simulator (AGHS). The AGHS adopts a hybrid RF/digital design that enables precision digital control of the GPS code and carrier signals. This allows coherent signal generation for simulations involving precise phase control, such as kinematic GPS testing, wavefront simulation, or ultra-tightly-coupled GPS/inertial testing.

Test results are presented in this paper showing the KCPT and Integrity Monitor performance under simulated conditions where interference sources, multipath sources and GPS/inertial failures are introduced.

INTRODUCTION

The Joint Precision Approach and Landing System (JPALS) Shipboard Relative GPS concept (SRGPS) is illustrated in Figure 1. The goal of the SRGPS program is to provide a GPS-based system capable of automatically landing an aircraft on a moving carrier under all sea and weather conditions considered feasible for shipboard landings. The presently utilized Aircraft Carrier Landing System (ACLS) is a radar-based system which was developed more than 30 years ago and has a number of limitations that make the system inadequate to meet present and future ship-based automatic landing system requirements. The goal of SRGPS is to monitor and control up to 100 aircraft simultaneously throughout a range of 200 nautical miles from the landing site[1]. Integrity monitoring is especially important for the last 20 nm of an approach and accuracy requirements are 30 cm 3-D 95% of the time.

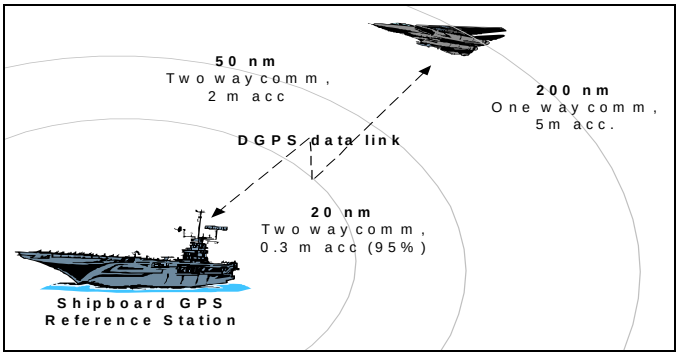

Figure 1 JPALS Shipboard Concept

The SRGPS architecture provides a precision approach and landing system capability for shipboard operations equivalent to local differential GPS systems used ashore,

such as the FAA's Local Area Augmentation System (LAAS). A relative navigation approach is used for SRGPS with the "reference station" installed on a ship moving through the water and pitching, rolling, and yawing around its center of motion. In addition, the ship's touchdown point may translate up/down (heave), side-to-side (sway), and fore and aft (surge). Since the shipboard landing environment is much more challenging than ashore, the SRGPS approach must use kinematic carrier phase tracking (KCPT) to achieve centimeter level positioning relative to the ship's touchdown point.

Next generation GPS systems designed for JPALS and SRGPS operations are expected to have performance advantages over previous generation user equipment (UE). While these designs will meet the objective of high anti-jam (A/J) and high accuracy performance, they must also implement integrity monitoring to be able to use the KCPT solution to support precision approach and landing.

KINEMATIC GPS INTEGRITY MONITORING

To achieve the high level of integrity needed for a KCPT solution to be used for precision approach and landing, the integrity monitoring approach shown in Figure 2 was designed. This includes the following three integrity monitoring components, each designed to detect failure modes that can affect the KCPT solution.

Spatial Integrity Monitor The purpose of the spatial integrity monitor (IM) is to detect errors in the receiver electronics or in the RF environment that can affect the GPS carrier phase observations used in the KCPT solution. This includes equipment or calibration errors that can affect the beamforming output, RF interference or multipath. The Spatial IM operates using built-in monitoring in the receiver spatial processing.

GPS/Inertial Integrity Monitor The GPS/inertial IM is used to detect GPS range or range rate errors that occur in the GPS observations. These errors can couple into the inertial navigation solution which is used to initialize the KCPT solution. With an ultra-tightly-coupled (UTC) GPS/inertial tracking implementation the inertial errors can also feed back directly into the carrier phase observations. The GPS/inertial IM operates using a Bounded Probability of Detection (BPOD) Receiver Autonomous Integrity Monitoring (RAIM) algorithm to detect faulty GPS data.

KCPT Integrity Monitor The KCPT IM is used to monitor for errors in the KCPT cycle ambiguities, caused either by cycle slips or incorrect ambiguity resolution. The KCPT IM operates on the set of carrier phase observations using a Fault Detection and Isolation algorithm combined with a real-time estimation algorithm for the Probability of Correct Detection of the KCPT ambiguities.

HAGR-A INTEGRITY TESTBED

The Kinematic GPS integrity monitoring algorithms were implemented and tested using NAVSYS High-gain Advanced GPS Receiver (HAGR) shown in Figure 3. This includes the electronics shown in Figure 4. The HAGR[2] is designed to accept inputs from a 7-element L1/L2 CRPA. Internally, the Digital Front-End (DFE) cards convert these inputs into the RF samples' digital signals. The Digital Beam Steering (DBS) cards include Field Programmable Gate Arrays (FPGAs) which create 12 L1 beams and 12 L2 beams each optimized for tracking a single GPS satellite. The Correlator Accelerator Card (CAC) includes the FPGAs which are used to track the individual satellite C/A and P(Y) codes under control of the host Pentium processor.

With the current generation analog controlled reception pattern antenna (CRPA) electronics in use by the DoD, a single composite RF signal is generated from the combined antenna inputs adapted to minimize any detected jammer signals. With next generation digital spatial processing GPS receiver designs, such as the HAGR, each antenna RF input is converted to a digital signal using a Digital Front-End. The DFE performs the function of phase-coherent down conversion and digitizing the received satellite RF signals. As illustrated in Figure 5, the DFE inputs from all of the antenna elements are then processed using spatial weights to create an optimized digital composite signal for each satellite tracking channel. The weights are created digitally and constrained to avoid introducing any code or carrier phase errors on the resulting combined signal[3].

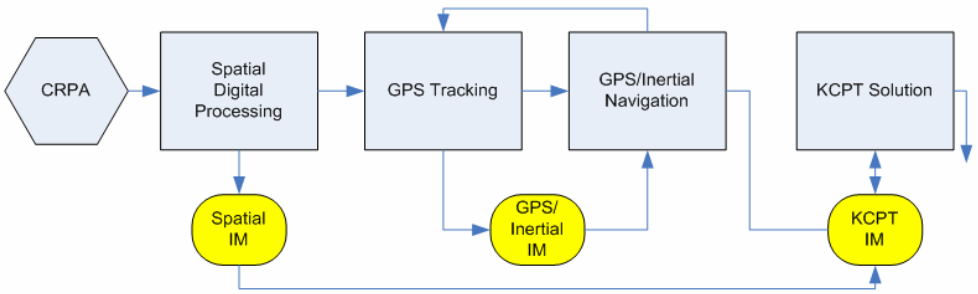

Figure 2 Integrity Monitoring Concept

The design of the integrity monitoring included in the HAGR and test results showing the performance of the Kinematic Integrity Monitoring are included in the following sections.

Figure 3 HAGR-A Digital Beamforming Receiver

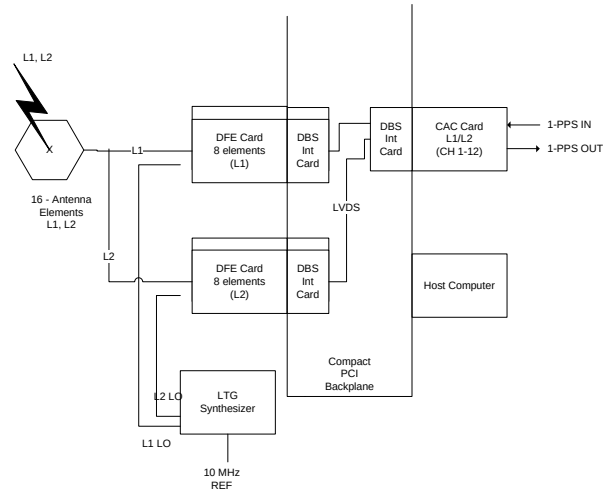

Figure 4 HAGR-A Components

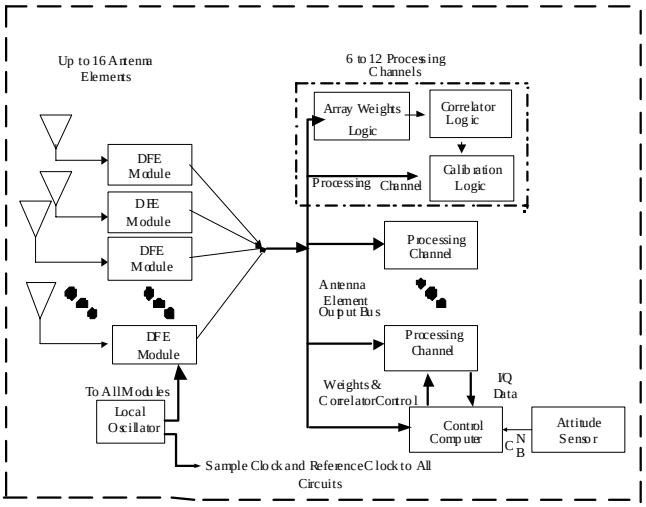

Figure 5 GPS Spatial Signal Processing

SPATIAL INTEGRITY MONITORING APPROACH

With conventional adaptive array processing, the combined signal is provided to the correlator channel for tracking. With digital beam/null-steering, the antenna patterns are optimized to minimize either the received jammer signal power or multipath signals, or both. The Spatial integrity monitoring function is designed to monitor both the pre-correlation and post-correlation spatial signal profiles. The pre-correlation power matrix is used to monitor for receiver electronics failures, such as DFE or local oscillator (LO) failures, and also to monitor for RF interference (RFI) sources. The post-correlation power matrix and calibration signals provide an estimate of the multipath spatial profile and the residual errors following RFI suppression.

Digital Front End Failure Detection

The operation of each individual DFE can be verified from monitoring the power of the cross-correlation terms relating to that element. If the DFE is operating correctly, then the diagonal elements of R should have the following relationship in Equation 1.

Equation 1

$$R_{ii} = N\sigma_n^2$$

By using a threshold test ($R_{ii} < T$), this can identify a faulty DFE output. This element can be removed from the total composite solution by setting its weight $w_i=0$.

Local Oscillator Failure

An LO failure will cause all of the DFE channels to cease operating. This can also be detected by monitoring the diagonal elements of the pre-correlation covariance matrix R.

Satellite Signal Multipath

Multipath errors are caused by the satellite signals being received from reflected surfaces around the antenna array. This will distort the code and carrier tracking and introduce errors into the receiver. This failure mode can best be detected through spatial processing to detect the angle of arrival of different multipath signals.

The residual effect of the multipath on the signals after applying the digital weights can be estimated from the calibration signals using Equation 2. This can also be used to provide a quality factor for the expected residual multipath errors on the receiver's code and carrier measurements.

Equation 2

$$\underline{\varepsilon} = (\underline{e}_s \underline{w}')\underline{s}_c - \underline{e}_s \hat{S}(t)$$

Using these signals, a post-correlation covariance may be computed. The effect of using the post-correlation covariance matrix is that the GPS signals, which lie well-below the noise floor before correlation (and these are typically unobservable in a pre-correlation spatial

correlation), are now observable due to the processing gain derived from performing the correlations, as demonstrated in Figure 6.

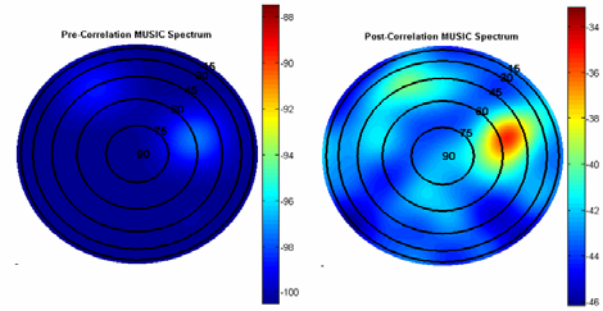

Figure 6 MUSIC Algorithm Results using Pre- and Post-Correlation Covariance Data

RF Interference

Although the effect of a GPS interference source can be mitigated using digital beam/null-steering, it can still degrade the accuracy of the GPS observations. High power continuous wave (CW) or pulsed signals can drive the DFE into saturation, suppressing the GPS signals. Broadband noise jammers have the effect of decreasing the satellite observed carrier-to-noise ratio (C/N0) which in turn increases the pseudorange and carrier phase tracking errors[4]. The post-correlation signal/noise can be estimated from knowledge of the pre-correlation covariance matrix, the applied beam/null-steering weights and the power spectral density of the jammer. The jammer/signal power is computed from Equation 3[4].

Equation 3

$$Js = \frac{\underline{w}' R \underline{w}}{\underline{w}' \underline{e}_{Si} \underline{e}_{Si}' \underline{w}}$$

The post-correlation signal/noise ratio can then be computed as follows in Equation 4. The scale factor Q=1 for a narrowband jammer and Q=2 for a broadband jammer.

Equation 4

$$Cn0 = \Pr - 10 * \log 10(kT + \frac{10^{(Js+\Pr)/10}}{fQ})$$

where

Cn0 is the signal/noise in dB-Hz
Pr is the nominal satellite power in dBw
kT is the Boltzmann's constant scaled
f is the chip spreading rate
Q is the jammer scale factor

SPATIAL INTEGRITY MONITOR TEST RESULTS

Our in-house AGHS simulator was used to simulate a variety of spatial integrity failure modes. A test was conducted that first simulated a series of DFE failures, followed by an LO failure, followed by the presence of a strong narrowband RF interferer. The diagonal values of the covariance matrix are shown in Figure 7, where the effects of all of these failures can easily be seen.

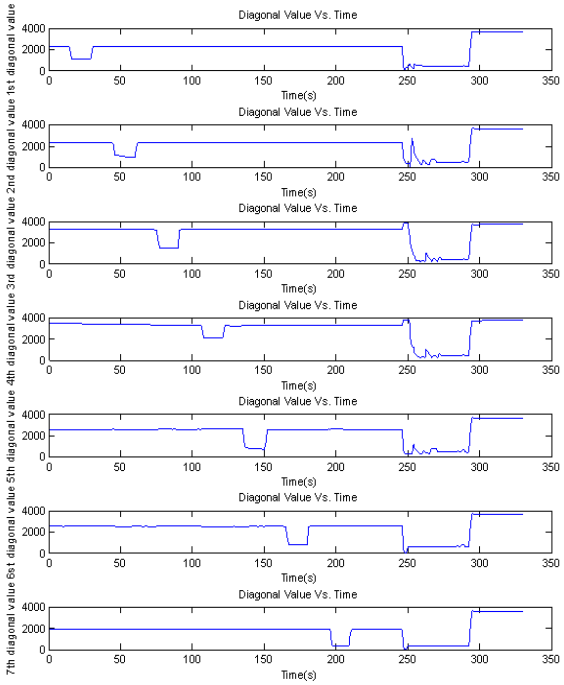

Figure 7 DFE and LO Failure Monitoring Results

A second test was performed to detect the presence of multipath interference and broadband RF interference. In this test a desired GPS signal was received at -30° azimuth, and a multipath reflection was received at 0°. Both the pre-correlation and post-correlation spatial covariance matrix were used to calculate the Capon spectrum, shown in Figure 8. Before correlation, both the direct path signal and the multipath reflection are so far below the noise floor that they do not appear in the Capon spectrum. Using the post-correlation spatial covariance matrix, they can both clearly be seen, and thus efforts can be taken to mitigate the effects of the multipath.

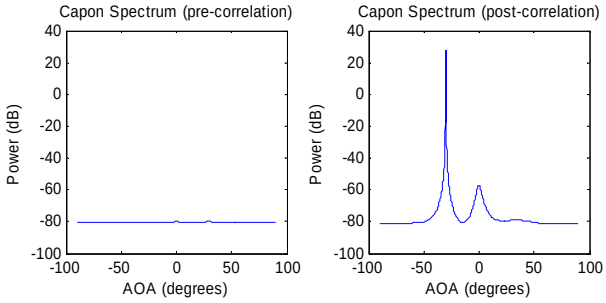

Figure 8 Pre- and Post-correlation Capon Spectrum Measurements

GPS/INERTIAL INTEGRITY MONITORING

The purpose of the GPS/Inertial integrity design is to detect any out of tolerance GPS faults from the blended solution before they are applied. This is to prevent corrupted GPS

data from propagating back into the GPS/Inertial solution. The GPS/Inertial Receiver Autonomous Integrity Monitor (GI-RAIM) algorithm is designed to detect faulty GPS observations provided to the inertial navigation Kalman filter. Unless the observations pass this high integrity test, they are not applied as measurement updates thus maintaining the integrity of the blended solution. The approach assumes that inertial systems will provide valid data over the short periods associated with final approach or that the plane will be waved off.

The GI-RAIM integrity algorithm is based on developing a set of conditional probabilities to assure detection of a satellite failure. This algorithm uses the "Bounded Probability of Missed Detection" (BPOD) approach developed by NAVSYS for the USCG[5] and USAF[6].

The GI-RAIM algorithm steps are shown in Figure 9, and the principle of operation of the BPOD algorithm is illustrated in Figure 10. When a satellite failure occurs, the position and velocity error distribution has a mean offset with the locus of position or velocity errors distributed around this mean in an ellipse. The magnitude of the ellipse is determined by the satellite geometry and the random noise on the solution.

If it can be determined correctly which satellite has failed, it is possible to use the redundant information to estimate the magnitude of the failure on that satellite. From this information, the expected error distribution of the solution resulting from the satellite failure can be predicted. Based on the given satellite geometry, a radius can be calculated that bounds the solution position error with a given Probability of Missed Detection (R_{PMD}). Conversely, we can also compute the threshold Radial Position Error (RPE) for the Horizontal Alert Level (HAL), R_T. If $R_{PMD} > R_T$, then a satellite failure has occurred which would exceed the HAL. A similar approach can be used for detecting vertical errors that exceed the Vertical Alarm Limit (VAL).

Table 1 BPOD Integrity Alarms

Alarm	Explanation
Red (*HDOP alarm*)	$RPE > RPE_{max}$ with probability > PMD_{max} and $PFA < PFA_{max}$ and B = 0
Purple (*BIAS alarm*)	$RPE > RPE_{max}$ with probability > PMD_{max} and $PFA < PFA_{max}$ and B≠ 0
Yellow	$RPE > RPE_{max}$ with probability > PMD_{max} and $PFA > PFA_{max}$
Green	$RPE < RPE_{max}$ and $PMD < PMD_{max}$

The BPOD algorithm sets integrity alarms based on the conditions shown in Table 1. A green alarm state indicates that no failures were detected. A yellow state indicates that the geometry was not sufficient for the BPOD algorithm to meet the integrity monitoring requirements. A purple state indicates that a satellite failure was detected and excluded. A red state indicates that the solution geometry exceeded the accuracy thresholds for navigation.

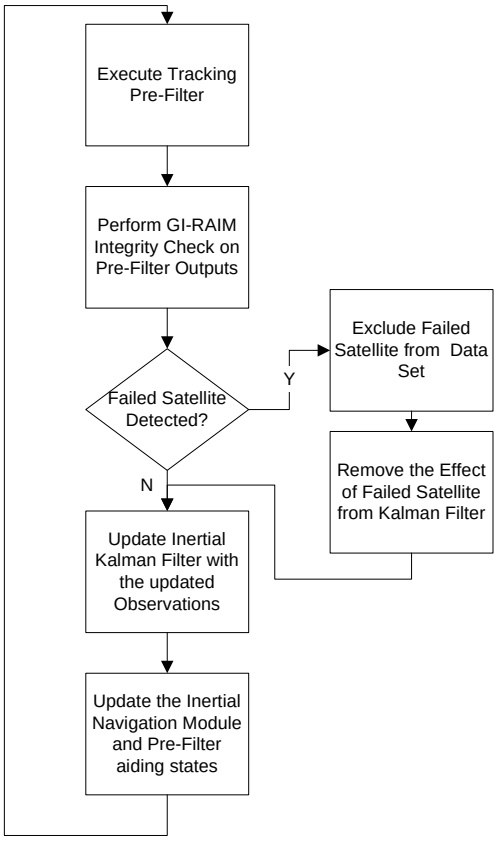

Figure 9 GI-RAIM Algorithm Steps

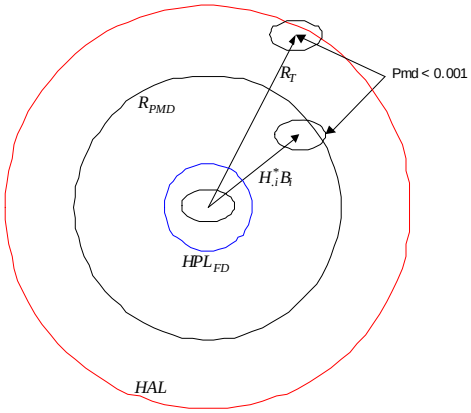

Figure 10 BPOD Principle of Operation

GI-RAIM TEST RESULTS

RTCA DO-299C and the JPALS SRD Revision 1 specify the following requirement for non-precision approach, as summarized in Figure 11. In order to test the ability of the proposed GI-RAIM algorithms to meet JPALS requirements

for non-precision approach, these figures were used to generate pseudorange and carrier phase thresholds for which the GI-RAIM algorithm uses to determine whether or not a satellite is out of tolerance and should be flagged.

	RTCA Non-Precision Approach [7]	**JPALS Non-Precision Approach [8]**
Accuracy	Horizontal Error (HE)< 100 m (95%)	Horizontal Error (HE)< 220 m (95%)
Alert Level	Horizontal Alert Level =480 m	Horizontal Alert Level =440 m
Missed Alert **False Alert** **Failed Exclusion** **Time-to-alert**	P(MA)≤0.001 P(FA)≤10-5/hr P(FE)≤0.001 TTA ≤ 10 sec	P(MA) ≤ 0.000005/hr P(FA) ≤ 0.00005/hr P(FE) = not defined TTA = not defined
Availability	Availability of Detection: 97.06% Availability of exclusion: 57.30%	Availability of Detection: not defined Availability of exclusion: not defined

Figure 11 Non-Precision Approach Requirements

The precision GPS/inertial simulation capability has been added to our Advanced GPS Hybrid Simulator (AGHS) product. This capability was first presented in [9], and has since been extended to support GI-RAIM testing for this effort. The AGHS was developed using software defined radio architecture to allow for detailed real-time software control of the waveforms and signals being generated. The AGHS can be configured to support different numbers of simulated satellite, platform and antenna configurations. The model shown in Figure 13 is capable of simulating 12 GPS satellites simultaneously, and can model any antenna array with up to 8 elements (L1 and L2).

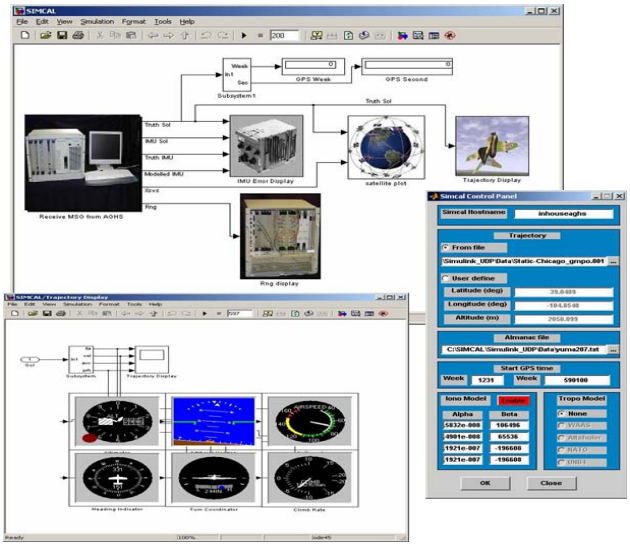

Figure 12 Simulink Control Software

An example of how multiple units can be connected, to simulate the SRGPS JPALS scenario, is shown in Figure 14. Here, two AGHS units are used, one to simulate the signals received at the ship-board units and provide the simulated inertial data provided by the ship's systems into the SRGPS Reference Receiver, and the second unit to simulate the signals received onboard the aircraft and to provide the simulated aircraft inertial data. The SRGPS Reference Receiver can compute the DGPS corrections in real-time and pass these up to the aircraft's receiver where they are applied. The AGHS units and HAGR receivers are also designed to interface in real-time with Simulink through the Ethernet network connection. This allows real-time insertion of modeled errors and also real-time collection and display of performance data throughout the test.

Figure 13 NAVSYS' Advanced GPS Hybrid Simulator

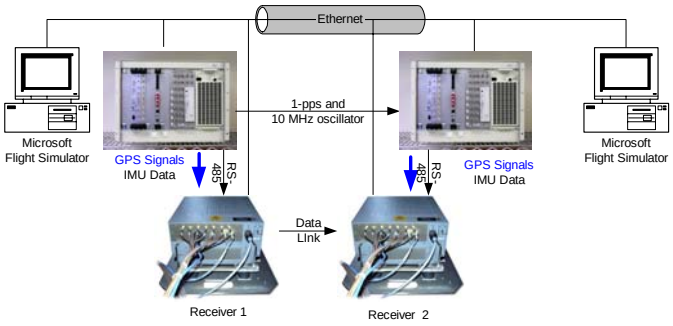

Figure 14 Example Test Configuration with Multiple AGHS Simulators

IMU data from a simulated LN100 and simulated GPS measurement with ramping effect (delta-range bias) were simulated (as shown in Table 2 and Figure 15). They are then processed by the GPS/INS GI-RAIM algorithm. Test results show that under JPALS non-precision approach requirement, 3cm/s ramping error can be detected. Figure 16 shows the RAIM test results for a certain epoch during the simulation. The purple dots show the detected delta-range errors and the green ones show the undetected delta-range errors with velocity errors within velocity-alarm-level (0.01 m/s in this case). Figure 17 shows the RAIM test results for the whole flight simulation. It can be seen that 6 out of 9 satellite ramping errors can be detected. The 3 ramping errors that were not detected did not cause the solution to exceed the specified alarm thresholds.

Table 2 Instrumental Error of a LN100 IMU

Instrument Error	Value	Units
Accelerometer Bias	25	micro-gee
Accelerometer Scale factor	50	ppm
Accelerometer misalignment	10	urad
Gyro Bias	0.003	deg/hr
Gyro scale factor	1	ppm
Gyro noise	0.0015	deg/Rt-hr

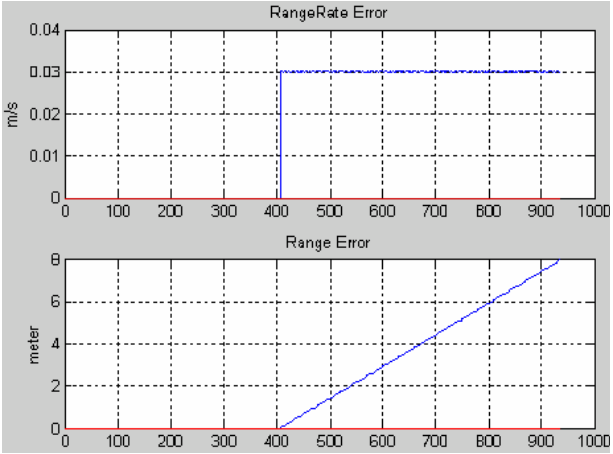

Figure 15 Simulated Ramping error of 3cm/s

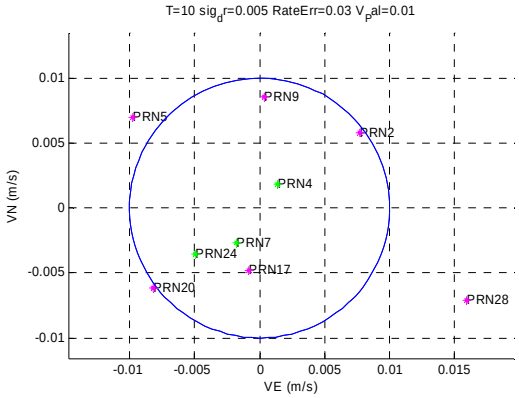

Figure 16 RAIM Results of 3cm/s Delta-Range Error Detection at a specific epoch

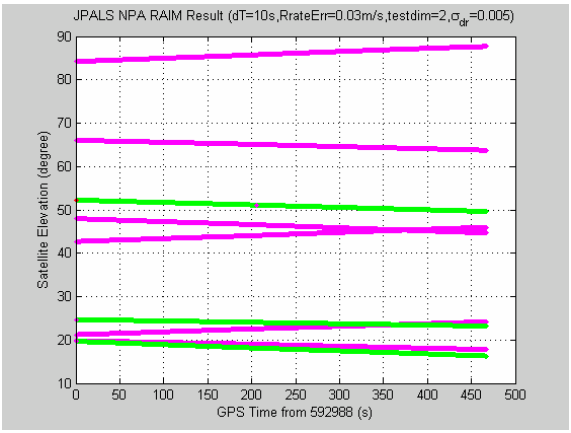

Figure 17 RAIM Results of 3cm/s Delta-Range Error Detection for the whole period of flight simulation

KCPT INTEGRITY MONITOR DESIGN

The purpose of the KCPT integrity monitoring test is to provide a confidence level for the ambiguity phase resolution of the kinematic GPS solution. In determining the ambiguity phase resolution, the integer number of carrier phase cycles from the antenna back to the satellite is estimated for all satellites tracked, as shown in Figure 18. If this is set correctly, then the KCPT position solution is accurate to the carrier phase noise, scaled by the solution geometry. If the carrier ambiguity is set incorrectly, then the KCPT solution is biased by the ambiguity error. In previous research, the ambiguity resolution approach has been derived based on white, Gaussian measurement noise assumptions[10]. For the SRGPS application, the measurement noise can be highly correlated due to multipath errors. The KCPT integrity monitoring algorithm is designed to use the Multipath/Signal (M/S) indication from the Spatial IM to estimate the effect of multipath errors on the ambiguity resolution and calculate a Probability of Correct Detection (PCD). Only when the PCD passes the IM threshold is the KCPT solution considered valid for a final approach.

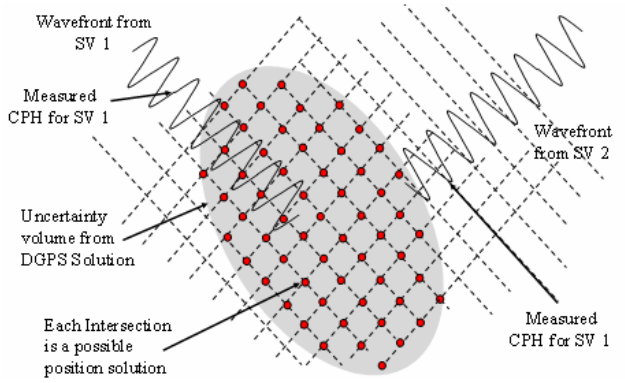

Figure 18 KCPT Ambiguity Phase Resolution

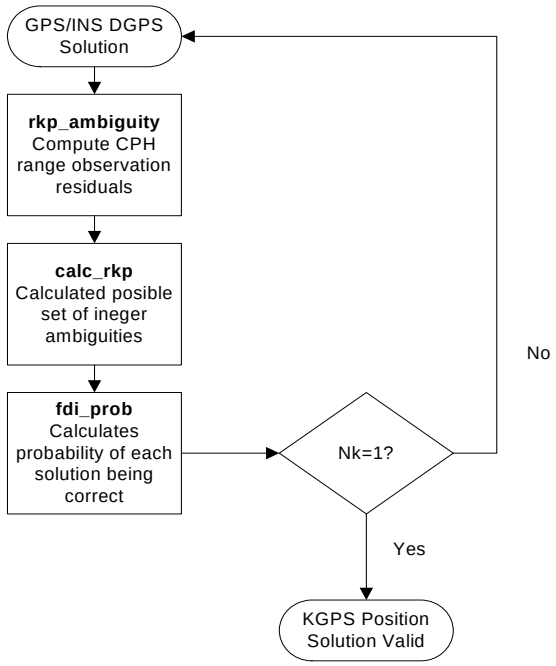

Figure 19 KCPT Ambiguity Resolution Steps

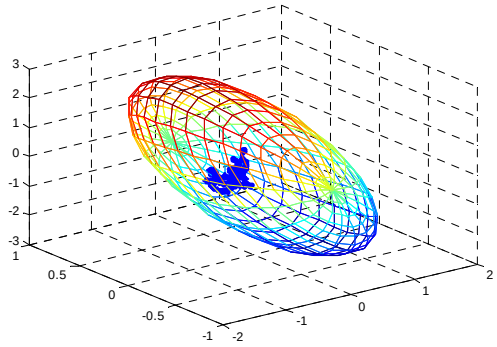

Figure 20 GPS/INS Kalman Filter Position relative to KGPS solution

The steps that the KCPT ambiguity resolution algorithm follows are shown in Figure 19. The initial search space for the ambiguity resolution process is defined by the GPS/inertial solution (Figure 20).

The selected ambiguity solutions are tested to identify the correct solution. The test metric that we have determined to be most reliable in terms of identifying the correct integer ambiguity in the presence of correlated noise is based on Equation 5. This selects the subset of valid ambiguity candidates based on the members of the test set that pass the following threshold.

Equation 5

$$F_0 = \sum_{k=1}^{n} (S_{t(k)}\vec{z}_{t(k)})^T (S_{t(k)}\vec{z}_{t(k)})$$

If the noise were purely Gaussian, then the correct Ambiguity has central (as shown in Equation 6) and others have non-central (as shown in Equation 7) chi-square distribution.

Equation 6

$$F_0 / \sigma^2_{cph} \sim \chi^2(Ndof, 0)$$

and

Equation 7

$$F_1 / \sigma^2_{cph} \sim \chi^2(Ndof, \lambda)$$

where

Equation 8

$$\lambda = E[F_1 - F_0]$$

An example fault vector distribution for both a correctly selected ambiguity and an incorrectly selected ambiguity is shown in Figure 21.

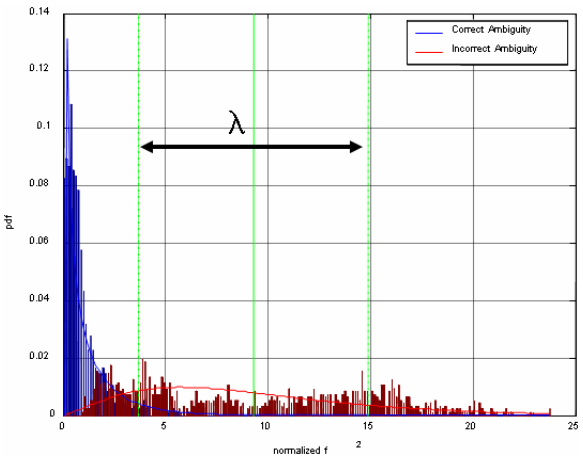

Figure 21 Example of Fault Vector Distribution

The probability of correct detection can be calculated from integrating over uncertainty in λ estimation which is a function of carrier phase noise, geometry and correlated multipath errors.

Equation 9

$$P_{cd} = \int_{-\infty}^{\infty} prob(F_0 < F_1 \cap F_0 < T) d\lambda$$

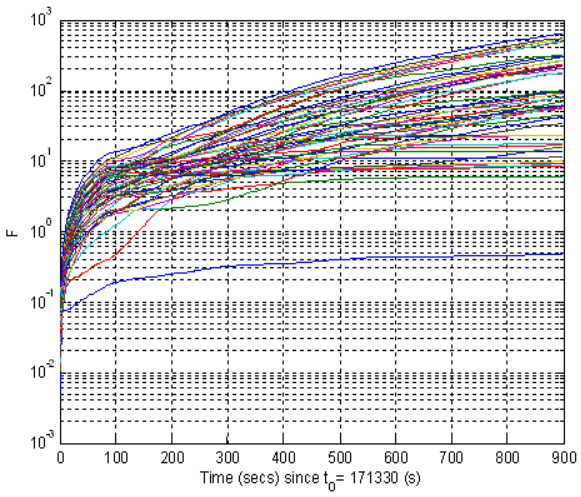

Figure 22 FDI Detection metric (F) of correct ambiguity

KCPT INTEGRITY MONITOR TEST RESULTS

The KCPT IM algorithm was validated using the AGHS test configuration described previously and also using live satellite data. Figure 23 shows a typical PCD curve for operations under normal conditions using live satellite data. It can be seen that the PCD for the selected ambiguity is above 99% for most of time, indicating the correctly ambiguity is selected. In Figure 24 the PCD is shown for a case when the ambiguity is not correctly initially selected. In this case, it can be seen that the PCD decreases over time.

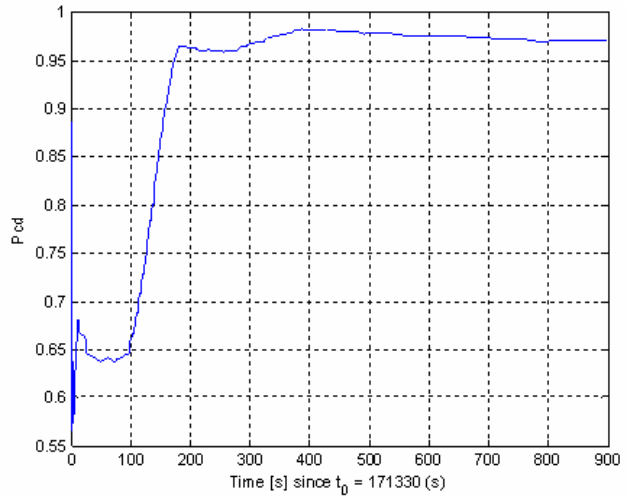

Figure 23 PCD for Correctly Selected Ambiguity Under Normal Conditions

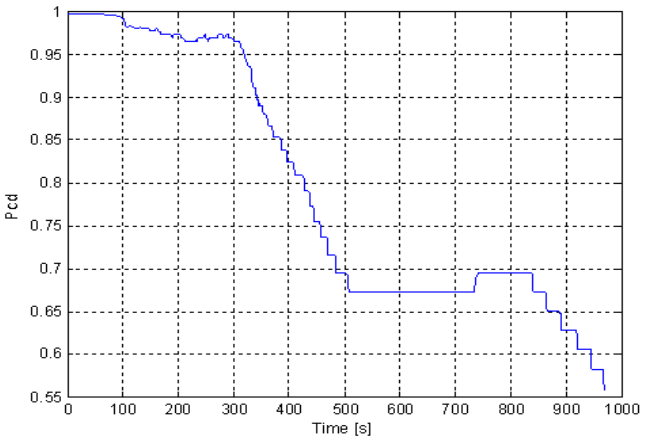

Figure 24 PCD for Incorrectly Selected Ambiguity Under Normal Conditions

The navigation solution quality and state information for the KCPT solution is shown in Figure 25 and Figure 26. The position error immediately falls to centimeter-level once the KCPT solution has been determined. The state information shown in Figure 26 is defined as follows:

State	Solution Type
0	No solution
1	Stand alone solution (Pseudo-range without DGPS corrections)
2	Differential solution (Pseudo-range and DGPS corrections)
3	Multiple kinematic solutions (Carrier-Phase and KGPS corrections)
4	Unique kinematic solution (Ambiguity resolved but Integrity check not yet passed)
5	Confirmed kinematic solution (PCD passed Integrity check threshold)

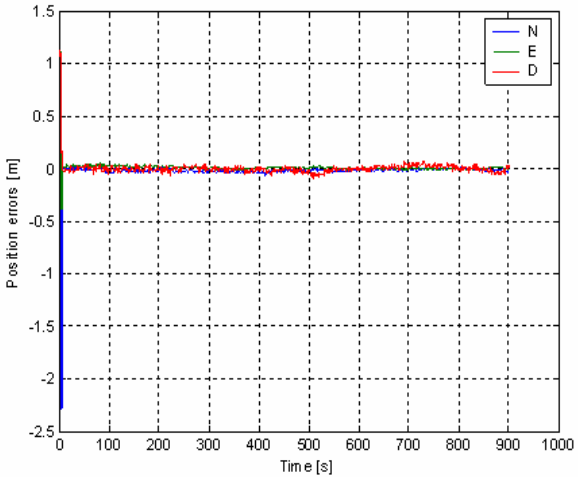

Figure 25 KCPT Solution Error

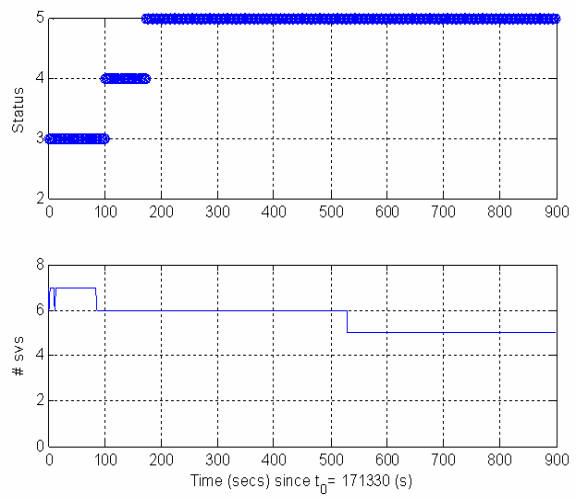

Figure 26 Solution State and Number of SVs Visible

A second test was conducted using data collected in the presence of a high amount of multipath interference. Figure 27 shows the PCD curve for this case. Due to the multipath, the kinematic integrity algorithm initially selected the incorrect ambiguity (State 4). However, the PCD correctly identified that due to the uncertainty introduced by the detected M/S level, the confidence of this ambiguity selection was below the integrity threshold. In this case, it took longer to verify the correct kinematic solution, but when the PCD passed the threshold the correct ambiguity had been identified. Navigation solution quality and state information for this case are shown in Figure 28 and Figure 29. As shown in this plot, selecting the incorrect ambiguity would have resulted in a significantly biased navigation solution.

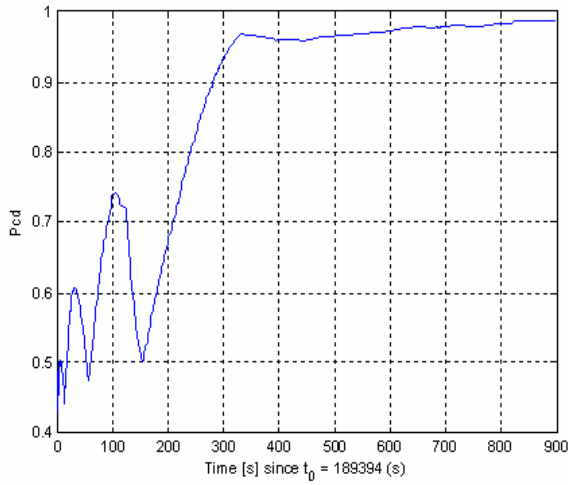

Figure 27 PCD for Correctly Selected Ambiguity High Multipath Conditions

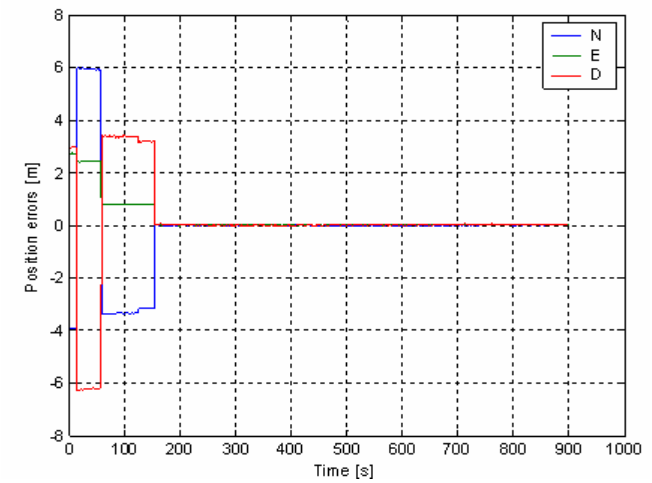

Figure 28 KCPT Solution Error

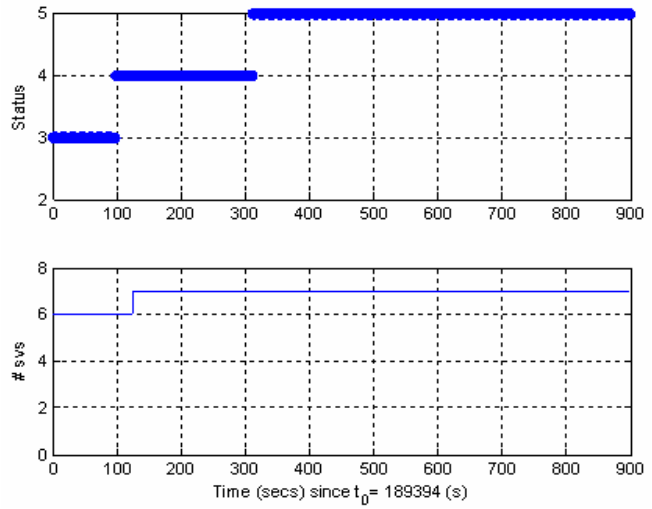

Figure 29 Solution State and Number of SVs Visible

CONCLUSIONS

The hybrid approach to Kinematic GPS integrity monitoring described in this paper presents a solution for detecting failure modes that can affect the final kinematic GPS solution accuracy in a precision approach and landing environment. The integrity monitoring algorithms described include Spatial IM to detect electronics failures and environmental effects, GPS/Inertial IM to detect faulty satellites, and KCPT GPS integrity monitoring to detect faulty ambiguity resolution. Hybrid Integrity Monitoring provides a robust, multifaceted approach to dealing with potential sources of error in precision navigation applications.

ACKNOWLEDGEMENT

The authors gratefully acknowledge the U.S. Navy's Naval Air Warfare Center for supporting this research. However, the views expressed in this paper belong to the authors alone and do not necessarily represent the position of any other organization or person.

REFERENCES

[1] System makes historic flight for naval aviation, "http://www.cnrma.navy.mil/news/june2001/2060701/2060701.html"

[2] A. Brown and R. Silva, "A GPS Digital Phased Array Antenna and Receiver," IEEE Phased Array Symposium, Dana Point, CA, May 2000

[3] A Brown and N. Gerein, NAVSYS Corporation, "Test Results of a Digital Beamforming GPS Receiver in a Jamming Environment," Proceedings of ION GPS 2001, Salt Lake City, Sept 2001.

[4] E. D. Kaplan, ed, "Understanding GPS Principles and Applications, Artech House Publishers, 1996.

[5] "Autonomous Failure Detection for Differential GPS," NAVSYS Document USCG 95-12.

[6] "GPS/IMU Ultra-Tightly Coupled Integrity Monitoring Final Report," NAVSYS Document No. GI-RAIM 02- 016, February 7, 2002

[7] "Minimum Operational Performance Standards for Global Positioning System/Wide Area Augmentation System Airborne Equipment," RTCA/DO-229C, November 28, 2001

[8] System Requirements Document (SRD) for Joint Precision Approach and Landing System (JPALS), 4 November 2005, US Naval Air Systems Command (NAVAIR)

[9] A Brown and B. Mathews, "Testing of Ultra-Tightly-Coupled GPS Operation Using a Precision GPS/Inertial Simulator," Proceedings of ION GNSS 2005, Long Beach, CA, Sept. 2005

[10] Teunissen, P.J.G., P.J. de Jonge, and C.C.J.M. Tiberius (1996) "The volume of the GPS ambiguity search space and its relevance for integer ambiguity resolution". Proceedings of ION GPS-96, 9th International Technical Meeting of the Satellite Division of the Institute of Navigation, Kansas City, Missouri, Sept. 17-20, pp. 889-898.